

Three new troglobitic *Coarazuphium* (Coleoptera, Carabidae, Zuphiini) species from a Brazilian hotspot of cave beetles: exploring how the environmental attributes of caves drive ground-beetle niches

Thais Giovannini Pellegrini^{1,2}, Rodrigo Lopes Ferreira³,
Robson de Almeida Zampaulo⁴, Letícia Vieira¹

1 Laboratório de Ecologia Florestal, Departamento de Ciências Florestais, Universidade Federal de Lavras, 37200-900 Lavras, Brazil **2** Departamento de Entomologia, Universidade Federal de Lavras, 37200-900 Lavras, Brazil **3** Centro de Estudos em Biologia Subterrânea (CEBS), Departamento de Biologia, Universidade Federal de Lavras, 37200-900 Lavras, Brazil **4** Gerência de Licenciamento Ambiental e Espeleologia, Vale S.A., Avenida Doutor Marco Paulo Simon Jardim, 34006-200 Nova Lima – Minas Gerais, Brazil

Corresponding author: Thais Giovannini Pellegrini (thais.g.pellegrini@gmail.com)

Academic editor: Srećko Čurčić | Received 18 August 2021 | Accepted 24 May 2022 | Published 10 June 2022

<http://zoobank.org/355BB7ED-D350-4DCD-990B-F6CC27D9C8D7>

Citation: Pellegrini TG, Ferreira RL, Zampaulo RdeA, Vieira L (2022) Three new troglobitic *Coarazuphium* (Coleoptera, Carabidae, Zuphiini) species from a Brazilian hotspot of cave beetles: exploring how the environmental attributes of caves drive ground-beetle niches. *Subterranean Biology* 43: 97–126. <https://doi.org/10.3897/subtbiol.43.73185>

Abstract

Three new species of troglobitic beetles of the genus *Coarazuphium* are described from specimens collected in iron ore caves in the Flona de Carajás in Brazil, doubling the number of known species for the Carajás region. The new species of *Coarazuphium* are morphologically similar to the already described species from the same region and are distributed in a small geographic range. From all *Coarazuphium* species of the region, including the new ones, two stand out, *C. spinifemur* and *C. xingu* **sp. nov.**, which are the smallest *Coarazuphium* species. Both species have shorter legs and antennae when compared to the others. The main characteristic that differentiates *C. xikrin* **sp. nov.** and *C. kayapo* **sp. nov.** from the other two species from the Carajás region, *C. tapiaguassu* and *C. amazonicum*, is that the new species have more numerous setigerous punctures dorsally on the head. With the three new species added to the six already described congeners, the area of intense mining of the Carajás region includes the highest diversity of obligatory cave-dwelling beetles in Brazil, representing a hotspot of cave beetles. *Coarazuphium xikrin* **sp. nov.** and *C. amazonicum* co-occur in some of the caves of the Carajás region, which is possible due to putative

niche differentiation between the species. These findings highlight the importance of maintaining legal provisions that ensure the preservation of caves, especially those most relevant regarding physical and biotic aspects, which is crucial for the conservation of Brazilian subterranean biodiversity.

Keywords

Amazon rainforest, Brazil, cave-restricted, endemic, iron ore, outlying mean index, sympatric species

Introduction

The genus *Coarazuphium* Gnaspini, Vanin & Godoy, 1998 is currently represented by 14 species in the Neotropics. All species of the genus are subterranean as they are found in distinct underground strata. Thirteen of the 14 species are troglobitic (i.e., restricted to the cave environment) and endemic to Brazilian caves (Pellegrini et al. 2022). Only one species, *C. whiteheadi* Ball & Shpeley, 2014, is non-troglobitic and occurs in hypogean habitats in the mountains of Oaxaca, Mexico. Almost 70% of *Coarazuphium* species are known from only one or two caves close to each other, which indicates their narrow endemism [*C. tessai* (Godoy & Vanin, 1990), *C. bezerra* Gnaspini, Vanin & Godoy, 1998, *C. cessaima* Gnaspini, Vanin & Godoy, 1998, *C. formoso* Pellegrini & Ferreira, 2011, *C. caatinga* Pellegrini & Ferreira, 2014, *C. ricardo* Bená & Vanin, 2014, *C. spinifemur* Pellegrini & Ferreira, 2017, *C. lundi* Pellegrini, Ferreira & Vieira, 2020, *C. auleri* Pellegrini & Vieira, 2021 and *C. bambui* Pellegrini & Vieira, 2022].

Most *Coarazuphium* species are associated with caves in carbonate formations (Pellegrini and Ferreira 2011). The only known species from iron ore caves are *C. spinifemur*, *C. tapiaguassu* Pellegrini & Ferreira, 2011 and *C. amazonicum* Pellegrini & Ferreira, 2017. The last two mentioned species have a broader distribution in different caves. The lower endemism in iron ore caves is a remarkable characteristic since most *Coarazuphium* species are rare, with a few occurrences or observations (Pellegrini et al. 2020). All *Coarazuphium* species associated with iron ore caves are endemic to the Carajás Mineral Province (southeastern Amazon, Brazil). This area possesses rich mineral resources and is currently considered a cave biodiversity hotspot with many endemic or threatened species and several undescribed taxa (Jaffé et al. 2016). So, it is a great challenge to balance the conservation of endemic or threatened species with mining activities and the interests of the local human population of the Carajás region (Jaffé et al. 2016).

Troglobitic species are target taxa for conservation and can guarantee total protection to caves depending on their rarity and spatial distribution pattern (Brasil 2017). The first step towards effective conservation of a given cave species is to ensure that the species is known to science and to determine its distribution throughout the caves and habitat preferences. Thus, understanding species' habitat preferences and niche occupation are essential information to build a reliable conservation plan to protect the species and their habitats (Barlas and Yamaç 2019). However, there are little information available about the environmental conditions and natural history of *Coarazuphium*. Most of the information on *Coarazuphium* species came from specimens gathered from zoological collections, and the only available data on these species is represented by their taxonomic descriptions.

On the other hand, the ferruginous caves from the Carajás National Forest database offer a unique opportunity to study the habitat preferences of these endemic and threatened species (Jaffé et al. 2018). The newly discovered species, *Coarazuphium xikrin* sp. nov., has a broad occurrence in Carajás caves, overlapping the distribution of *C. amazonicum*. In this study, we tested the hypothesis that niche differentiation makes the coexistence of these *Coarazuphium* species possible. Evidence supports our hypothesis that in a habitat with scarce resources the coexistence of ecologically similar species is possible when traits exhibit subtle differences (Violle et al. 2011). The absence of such differences may result in competitive exclusion of recently diverged species (Webb et al. 2002). Thus, niche differentiation would reduce the interspecific competition promoting the species coexistence (Dayan and Simberloff 2005; Mayfield and Levine 2010). In particular, caves possess harsh environmental conditions that works as a highly selective ecological filter for the species pool (Mammola et al. 2016). The coexistence of *Coarazuphium xikrin* sp. nov. and *C. amazonicum* offers the opportunity to investigate the niche differentiation among them. Therefore, the main purpose of the present study is to describe three new species of *Coarazuphium* to science from Brazilian iron ore caves in the Carajás Mineral Province. Additionally, we performed the ecological niche modeling between two of the most abundant *Coarazuphium* species with co-occurrence in the caves of Carajás. Finally, we provide a key to aid species identification within the genus *Coarazuphium*.

Materials and methods

Study area

The three new species described in this work occur in caves in the eastern region of the Amazon Forest in the state of Pará, Brazil (Figs 2, 4–7). Two of them are associated with ferruginous caves in the Carajás National Forest (Flona de Carajás) – one in the Serra Norte area and the other in the Serra Sul area. The National Forest of Carajás encompasses approximately 411 thousand hectares and includes parts of the municipalities of Parauapebas, Canaã dos Carajás, and Água Azul do Norte. The National Forest of Carajás is a mosaic of protected areas forming a continuous area of 1.31 million hectares of preserved forests (Rolim et al. 2006) surrounded by cattle farmland (Campos and Castilho 2012; Martins et al. 2012). The park area mainly comprises forest formations (ombrophilous or seasonal), with only 5% consisting of rocky/rupestrian fields, which develop on the laterite plates (crusts) of high areas of the region (Campos and Castilho 2012). The third new species described in the current study was found in an iron ore cave located in the municipality of São Felix do Xingu. The metavolcanic-sedimentary sequence from the São Félix Group (also of iron-ore lithology) occurs in the extreme southwest of the Carajás Domain (Valentim and Olivito 2011; Ferreira and Lamarão 2013). There are currently 88 caves registered in this region according to the Brazilian National Register of Speleological Information database – CANIE (CECAV 2021), all in iron ore formations, and the area, unlike the Carajás National Forest, is highly altered by illegal mining, farming and illegal deforestation (Mertens et al. 2002; Souza-Filho et al. 2016; Oliveira et al. 2020; Rizzo et al. 2020).

Methods

All adult specimens used in this study were obtained from the Museu de Zoologia da Universidade de São Paulo, São Paulo (MZSP) and the Coleção de Invertebrados Subterrâneos da Universidade Federal de Lavras, Lavras, Minas Gerais (ISLA). A part of the material is stored in vials containing 70% ethanol, while other specimens are dried and fixed on entomological pins. Morphological observations were made using a Stemi 508 stereomicroscope (Carl Zeiss, Germany), while measurements and photographs were obtained using an AxioCam 506 color camera (Carl Zeiss, Germany) connected to an Axio Zoom V16 stereomicroscope (Carl Zeiss, Germany).

Fine entomological pins were used to dissect insect specimens and extract male and female genitalia. Male genitalia were treated with pancreatin to clear the soft tissues. We followed procedures for female genitalia modified after Liebherr (2015). Briefly, we first removed the entire female abdomen. The abdomen was then treated with an aqueous solution of cold 10% potassium hydroxide (KOH) overnight. The female reproductive tract was placed in glycerin and isolated from other abdominal structures first by tearing off the membranous tergites followed by removal of the digestive tract and tracheal system, and finally removing the ventrites. We then mounted the female reproductive tract on glass slides in Kayser glycerol gelatin using standard procedures developed for mites (Walter and Krantz 2009). Observations and imaging of female genitalia were made using a DM750 microscope (Leica, Germany) and an Axio Zoom V16 stereomicroscope (Carl Zeiss, Germany).

All figures were edited using the Adobe Photoshop CS5 software, version 12.0. The use of terms for male and female genital structures follows Ball and Shpeley (2013) and Liebherr and Will (1998). All measurements are in millimeters (mm).

Abbreviations of body measurements and structures

A1L	scape length;
A2–4L	length of antennomeres 1–3 combined;
AL	antennal length from the base of the scape to the tip of the 10 th antennomere;
ASOS	anterior supraorbital setigerous punctures;
EL	elytral length (linear distance from the humerus to the apex);
EW	maximum elytral width (the longest linear transverse distance);
HL	head length (linear distance from the apex of the clypeus to the posterior margin of the postociput);
HW	head width (maximum transverse distance across head, including eyes);
HWL	length of hind wings (the longest linear transverse distance);
OBL	overall body length (the sum of HL, PL, and EL);
OCS	occipital setigerous punctures;
PL	pronotum length (linear distance from the anterior margin to the posterior margin measured along the midline);

- POS** postocular setigerous punctures;
PSOS posterior supraorbital setigerous punctures;
PSUS posterior supernumerary setigerous punctures;
PW maximum pronotum width (the longest linear transverse distance) (Fig. 1).

Abbreviations of male genital structures

- GSL** genital segment length;
GSW genital segment width;
LPL left paramere length;
MLA length of median lobe of aedeagus (measured in a straight line from the basal margin to the apical margin);
OML peristial membrane length (measured in a straight line from the basal margin to the apical margin);
RPL right paramere length.

It is worth mentioning that in most Carabidae, the aedeagus has a 180° torsion in an active situation (Deuve 1993). By convention, in this paper what is called ventral is anatomically dorsal, what appears right is anatomically left, and what appears left is anatomically right.

Cave physical characteristics and organic resources

Data on the physical characteristics and organic resources of the sampled caves were obtained by consulting companies that employed standardized methods for the same set of cave attributes (for more details see the Brazilian legislation for the protection of caves:

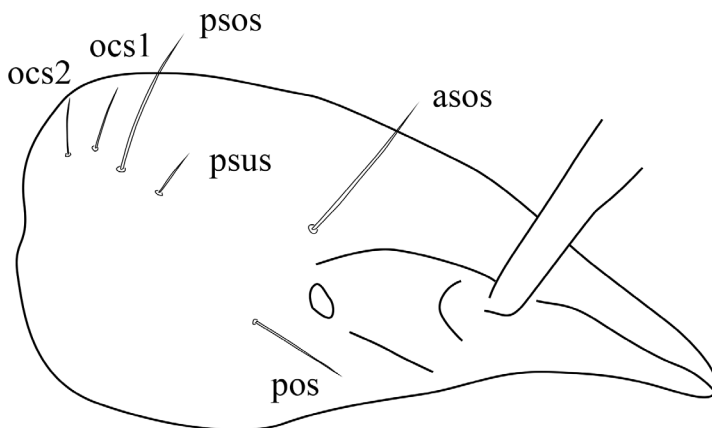
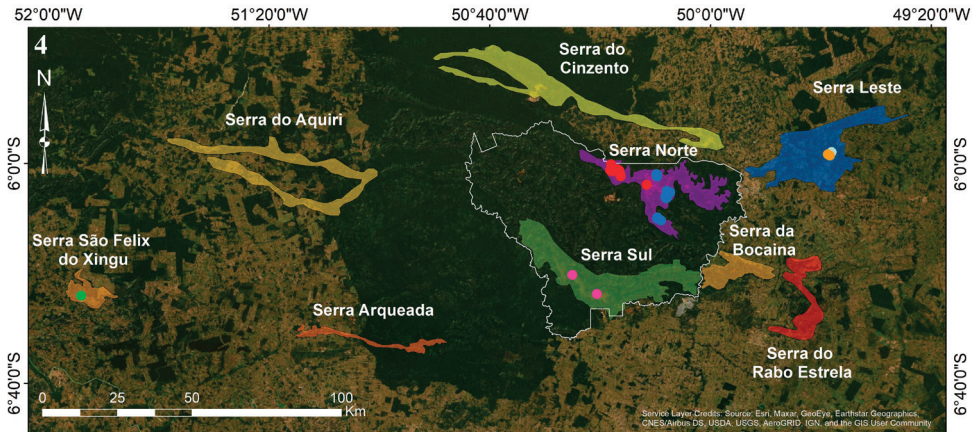
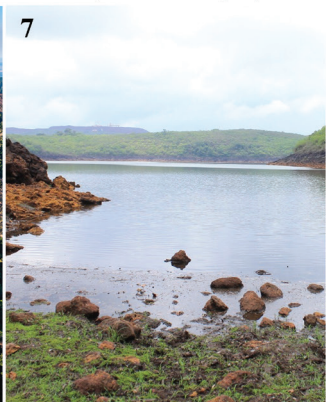


Figure 1. A schematic representation of setigerous punctures distribution on the head (lateral view) in *Coarazuphium* species. For codes interpretation see the Materials and methods section.



● *C. amazonicum* ● *C. kaiapo* sp. nov. ● *C. spinifemur* ● *C. tapiaguassu* ● *C. xikrin* sp. nov. ● *C. xingu* sp. nov.



Federal Decree 6640/2008 and Normative Instruction MMA 02/2017) (Brasil 2008, 2017). The cave characteristics included the following data: GPS coordinates, altitude (taken at the cave entrance), horizontal projection (length), slope, area, volume (these last four parameters were obtained from the cave maps), and the presence of percolating water or water reservoirs (e.g., puddles or lakes). The organic resources recorded included the presence of plant debris, organic detritus, roots, guano, feces from vertebrates other than bats, and regurgitation balls from owls and carcasses. These organic resource variables were not evaluated separately, but were analyzed together to calculate the diversity of organic matter resources available using Shannon's diversity index.

Data analyses

To evaluate the marginal use of the available habitat by two sympatric species (*Coarazuphium amazonicum* and *C. xikrin* sp. nov.), we performed the outlying mean index (OMI). OMI is a multivariate technique that measures the distance between the mean values used and the mean values available for each environmental condition of the total sampled area (Dolédec et al. 2000). This analysis provides information on niche marginality (average distance of the hypervolume centroid – OMI), tolerance values (niche width – Tol), and residual tolerance (variation of niche width that was not related to the studied variables – Rtol). In addition, it calculates the total inertia that estimates the influence of environmental variables on niche separation (Dolédec et al. 2000).

The cave characteristics and organic matter diversity measures mentioned above were standardized to a mean of 0 and a standard deviation equal to 1 in order to make the scales comparable. All available adult specimens of *C. amazonicum* (27) and *C. xikrin* sp. nov. (33) were included in this analysis to improve model accuracy. The analysis was performed using the R software, version 3.6.2 (R Core Team 2019) utilizing the “ade4” package (Dray and Dufour 2007). The Monte Carlo test with 10,000 permutations was used to evaluate the significance of niche marginality and the average marginality of species (Dolédec et al. 2000).

Figures 2–7. Geographic distribution of *C. xikrin* sp. nov., *C. kayapo* sp. nov. and *C. xingu* sp. nov. **2** location of the caves with occurrences of the new species in the state of Pará, Brazil and South America **3** *Coarazuphium kayapo* sp. nov., a living specimen **4** location of the caves (circles) where *Coarazuphium* species have been collected. Shaded regions correspond to the different highlands in the area **5** photograph of the São Félix do Xingu region, where is situated the type locality (Cave SFX-0057) of *C. xingu* sp. nov. **6** photograph of the N1N8 area from the Serra Norte highland, where most of caves with occurrences of *C. xikrin* sp. nov. are located **7** photograph of a lake found in the Serra Sul highland, where caves with occurrences of *C. kayapo* sp. nov. are located. Photo credits: Ativo Ambiental (**3**), Fundação Casa de Cultura de Marabá (**5**), Marcelo Rosa (**6**), and Robson de Almeida Zampaulo (**7**).

Results

Order Coleoptera Linnaeus, 1758

Family Carabidae Latreille, 1802

Tribe Zuphiini Bonelli, 1810

Genus *Coarazuphium* Gnaspini, Vanin & Godoy, 1998

Coarazuphium xikrin Pellegrini, Ferreira & Vieira, sp. nov.

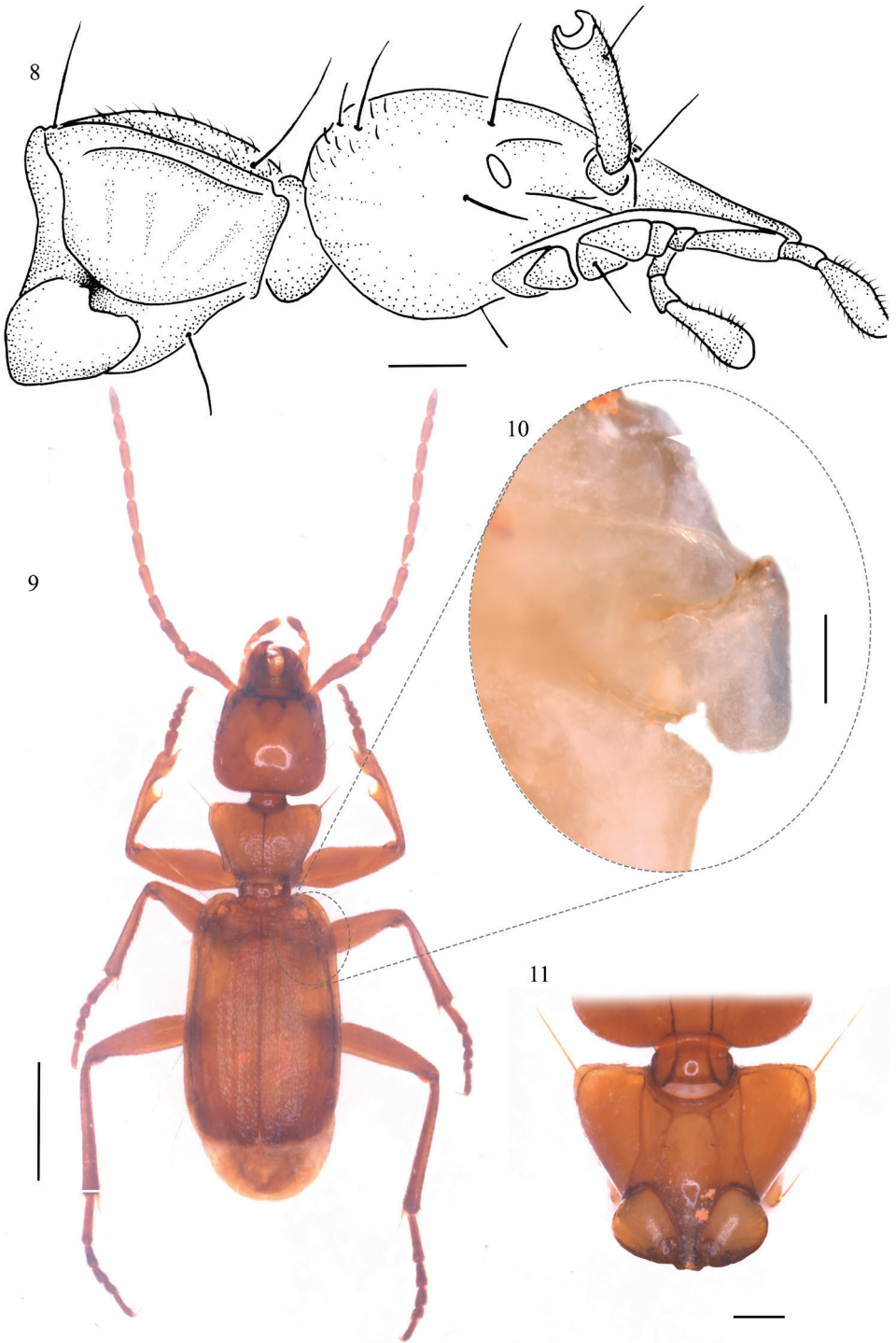
<http://zoobank.org/0BB32336-7C52-477A-A44D-7466B7C6AE7D>

Figs 8–17

Type material. *Holotype*: BRAZIL: Pará, Serra dos Carajás, Cave N1N8/N1-0020 Flona Carajás, PA, 6°01'57.7"S, 50°16'18.6"W, 639 m a.s.l., ♂, 17.VII–04.VIII.2014, Carste Company leg. (MZSP49180).

Paratypes (10 specimens). BRAZIL: Pará, Serra dos Carajás, Cave N1N8/N1-0022 Flona Carajás, PA, 6°01'57.0"S, 50°16'18.6"W, 642 m a.s.l., 1 ♀, 17.VII–04.VIII.2014, Carste Company leg. (MZSP49181); the same locality as for preceding, 1 ♂, 17.VII–04.VIII.2014, Carste Company leg. (MZSP49182); BRAZIL: Pará, Serra dos Carajás, Cave N1N8/N1-0008 Flona Carajás, PA, 6°02'19.9"S, 50°16'13.1"W, 700 m a.s.l., 1 ♀, 24.II–13.III.2015, Carste Company leg. (MZSP49183); BRAZIL: Pará, Serra dos Carajás, Cave N1N8/N1-0073 Flona Carajás, PA, 6°01'13.5"S, 50°17'17.4"W, 507 m a.s.l., 1 ♀, 02–29.IV.2015, Carste Company leg. (MZSP49184); BRAZIL: Pará, Serra dos Carajás, Cave N1N8/N1-0037 Flona Carajás, PA, 6°01'49.9"S, 50°16'27.7"W, 723 m a.s.l., 1 ♂, 24.II–13.III.2015, Carste Company leg. (MZSP49185); BRAZIL: Pará, Serra dos Carajás, Cave N1N8/N1-0016 Flona Carajás, PA, 6°01'09.7"S, 50°16'40.9"W, 531 m a.s.l., 1 ♂, 04.IX–06.X.2014, Carste Company leg. (MZSP49186); BRAZIL: Pará, Serra dos Carajás, Cave N1N8/N1-0168 Flona Carajás, PA, 6°01'16.3"S, 50°18'05.1"W, 675 m a.s.l., 1 ♂, 17.VII–04.VIII.2014, Carste Company leg. (MZSP49187); BRAZIL: Pará, Serra dos Carajás, Cave N1N8/N1-0240 Flona Carajás, PA, 6°01'18.5"S, 50°16'26.1"W, 638 m a.s.l., 1 ♀, 04.IX–06.X.2014, Carste Company leg. (MZSP49188); BRAZIL: Pará, Serra dos Carajás, Cave N1N8/N1-0101 Flona Carajás, PA, 6°01'08.7"S, 50°16'46.2"W, 541 m a.s.l., 1 ♀, 04.IX–06.X.2014, Carste Company leg. (MZSP49189); Cave N1N8/N1-0037 Flona Carajás, PA, 6°01'49.9"S, 50°16'27.7"W, 723 m a.s.l., 1 ♀, 04.IX–06.X.2014, Carste Company leg. (MZSP49190).

Additional material examined (seven specimens). BRAZIL: Pará, Serra dos Carajás, Cave N1N8/N1-0062 Flona Carajás, PA, 6°01'09.6"S, 50°16'44.4"W, 533 m a.s.l., 1 ♀, 04.IX–06.X.2014, Carste Company leg. (MZSP49191); BRAZIL: Pará, Serra dos Carajás, Cave N1N8/N1-0016 Flona Carajás, PA, 6°01'09.7"S, 50°16'41.0"W, 535 m a.s.l., 1 ♀, 04.IX–06.X.2014, Carste Company leg. (MZSP49192); BRAZIL: Pará, Serra dos Carajás, Cave N1N8/N1-0240 Flona Carajás, PA, 6°01'18.5"S, 50°16'26.1"W, 599 m a.s.l., 1 ♀, 04.IX–06.X.2014, Carste Company leg. (MZSP49193); the same locality as for preceding, 1 ♂, 02–29.IV.2015, Carste Company leg. (MZSP49194); BRAZIL: Pará, Serra dos Carajás, Cave N1N8/N1-0025 Flona Carajás, PA,



Figures 8–11. *Coarazuphium xikrin* sp. nov., external morphology **8** head and prothorax, lateral view **9** habitus, dorsal view **10** a detail of hind wings, dorsal view **11** prothorax, ventral view. Scale bars: 1.0 mm (**9**); 0.5 mm (**8**); 0.2 mm (**11**); 0.1 mm (**10**).

6°01'49.5"S, 50°16'19.8"W, 621 m a.s.l., 1 ♀, 02–29.IV.2015, Carste Company leg. (MZSP49195); BRAZIL: Pará, Serra dos Carajás, Cave N1N8/N1-0037 Flona Carajás, PA, 6°01'49.9"S, 50°16'27.7"W, 723 m a.s.l., 1 ♀, 04.IX–06.X.2014, Carste Company leg. (MZSP49196); BRAZIL: Pará, Serra dos Carajás, Cave N1N8/N1-0052 Flona Carajás, PA, 6°01'49.5"S, 50°16'19.8"W, 771 m a.s.l., 1 ♀, 24.II–13.III.2015, Carste Company leg. (MZSP49197).

Etymology. The species name honors the Xikrin ethnic group (Brazilian Indians), which live in the Carajás region. The Xikrin Indians speak the Kayapó language, which emphasizes listening and speaking. To sharpen these qualities, the Xikrin pierce, as early as infancy, the corresponding organs (ears and lips). For this ethnic group, listening is related to knowing, to acquiring knowledge. Oral communication, in turn, is a highly valued social practice for the Kayapó groups in general, who define themselves as those who speak well and beautifully. This noun should be treated as in apposition.

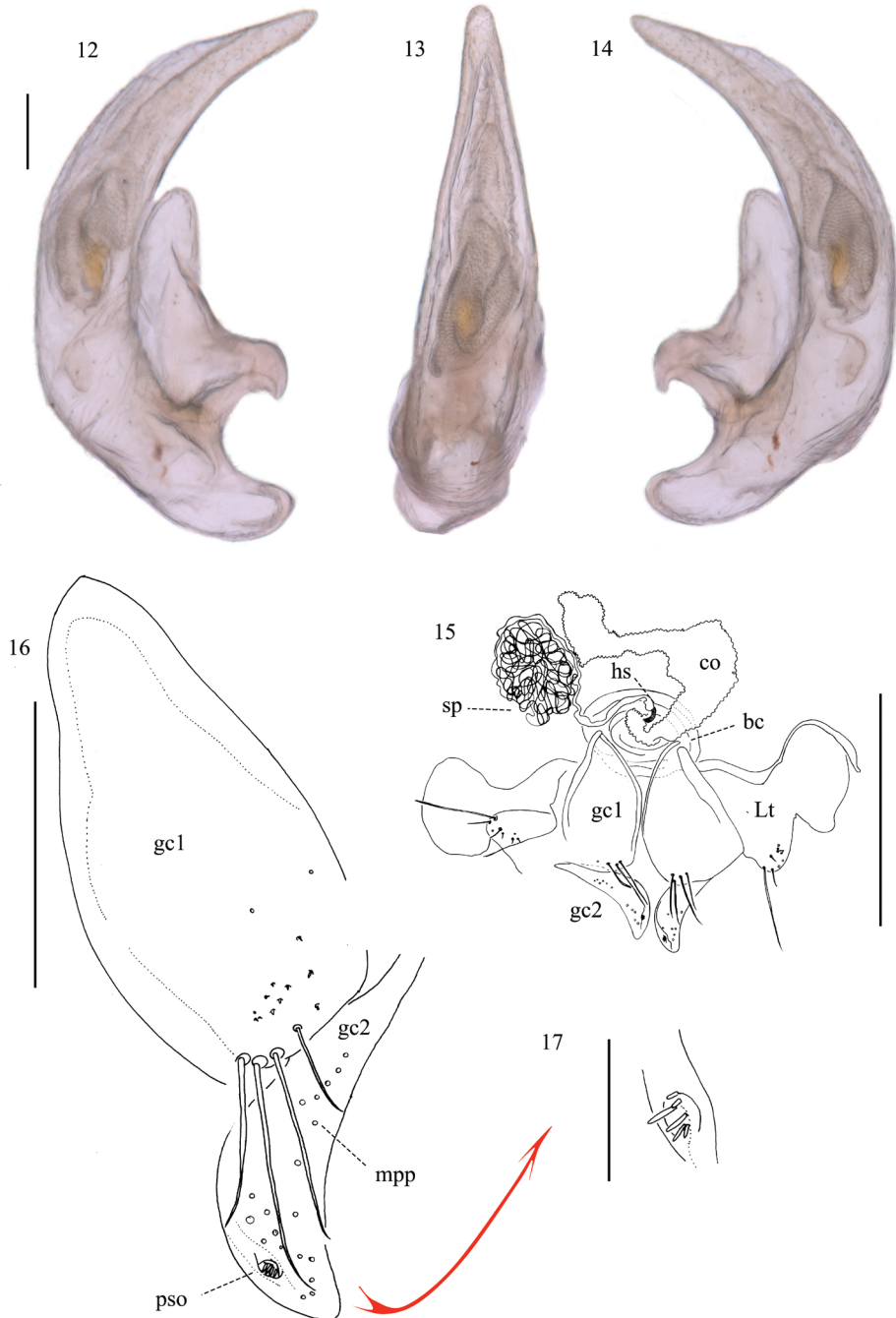
Differential diagnosis. All characteristics of *C. xikrin* sp. nov. are consistent with the description of the genus *Coarazuphium*. This species differs from all other members of the genus by the following combination of characters: elytral outline subparallel, elytra with maximum width in the posterior half, with apical margin truncate, without subapical sinuosity; location of setigerous punctures on the head dorsally: one pair of anterior supraorbital, one pair of postocular, one pair of posterior supraorbital and one pair of occipital; metafemur without a spine medially at its ventral side; antennae long, about 0.80 times as long as body length; median lobe of aedeagus about 2.81 as long as left paramere and 4.55 as long as right paramere.

Description. Size and proportions. OBL: 3.89 mm (3.82–3.99 mm ♂♂, 3.79–4.06 mm ♀♀); EW: 1.36 mm (1.27–1.39 mm ♂♂, 1.29–1.45 mm ♀♀); HW/PW: 0.99 (0.99–1.02 ♂♂, 1.04–1.09 ♀♀).

Habitus. Body with uniform pale to dark brown color (Fig. 9).

Integument. Dorsally covered with short recumbent hairs.

Head. Subtrapezoidal (Fig. 9), HW/HL: 0.93 (0.87–0.95 ♂♂, 0.89–0.98 ♀♀). Head almost as wide as pronotum. Setigerous punctures on the head dorsally: one pair of anterior supraorbital above the eyes; one pair of postocular immediately behind the eyes, laterally; one pair of posterior supraorbital posterior to the eyes; and one pair of occipital in the posterior margin of the head. There is also a pubescence evenly distributed on the head. The pubescence bristles are slightly bigger on the vertex of the head. Ventrally are four pairs of setae, three close to the gular region and the other located lateromedially (Fig. 8). Eyes reduced, depigmented, and flattened, situated laterally at the end of the genal sulcus, ommatidia are not visible at 50×. Antennae filiform and flagellar (Fig. 9), AL: 3.10 mm (3.08–3.18 mm ♂♂, 3.00–3.16 mm ♀♀), AL/PL: 4.89 (4.69–5.13 ♂♂, 4.58–4.97 ♀♀), A1L/A2–4L: 0.73 (0.75–0.86 ♂♂, 0.75–0.88 ♀♀), of almost the same length in both genders. First antennomere (scape) with a long seta distally close to the apical portion and a row of several semi-erect setae; 2nd one very short. Third antennal segment elongate, antennal segments 4–10 subequal and almost round in cross-section, except for the tip of the terminal antennomere, which is laterally flattened.



Figures 12–17. *Coarazuphium xikrin* sp. nov., male and female genitalia **12** aedeagus, left lateral view **13** aedeagus, dorsal view **14** aedeagus, right lateral view **15** female reproductive tract, dorsal view **16** gonocoxite, dorsal view **17** preapical setose organ, dorsal view **bc** bursa copulatrix **co** common oviduct **gc1** gonocoxite 1 **gc2** gonocoxite 2 **hs** helminthoid sclerite **Lt** laterotergite **mpp** marginal pit pegs **pso** preapical setose organ **sp** spermatheca **spg** spermathecal gland **spgd** spermathecal gland duct. Scale bars: 0.5 mm (**15**, **17**); 0.125 mm (**16**); 0.1 mm (**12–14**).

Prothorax. Pronotum trapezoidal, PL/PW: 0.65 (0.63–0.70 ♂♂, 0.65–0.70 ♀♀) (Figs 8, 9). Maximum pronotum width closely behind the anterior margin, which is almost as wide as the head. Anterior angle rounded. Posterior angle acute. Dorsal surface with two pairs of lateral marginal erect setae: one very long (0.8 times as long as pronotum), close to the antero-lateral angles, and the other shorter (0.5 times as long as pronotum), close to the postero-lateral angles. Prosternum with a pair of submedial setae (Figs 8, 11).

Pterothorax. Metasternum longer than wide. Metepisternum wider than long.

Elytra and hind wings. Elytra are free, with almost parallel sides (Fig. 9), EL/EW: 1.61 (1.56–0.70 ♂♂, 1.49–1.68 ♀♀). Maximum elytral width in the posterior third, EW/PW: 1.40 (1.34–1.50 ♂♂, 1.38–1.52 ♀♀). Elytral apex is truncate, not sinuate. Elytral chaetotaxy: no discal setae present; the umbilicate series of the 8th stria with seven large setae (about 0.58 as long as elytra) on each elytron, situated as follows: three close to the anterior angle, two marginal in the lateral posterior half, and two on the posterior margin. Hind wings very reduced (Fig. 10), 0.204-mm long, HWL/EL: 0.09.

Legs. Profemur 1.05 (1.02–1.13 ♂♂, 1.03–1.20 ♀♀) times as long as mesofemur and 0.75 (0.70–0.77 ♂♂, 0.68–0.77 ♀♀) times as long as metafemur. Protibia 1.20 (1.02–1.20 ♂♂, 1.02–1.19 ♀♀) times as long as mesotibia and 0.77 (0.65–0.76 ♂♂, 0.69–0.79 ♀♀) times as long as metatibia. Protibia 1.33 (1.16–1.35 ♂♂, 1.20–1.43 ♀♀) times as long as protarsus. Mesotibia 0.85 (0.89–0.98 ♂♂, 0.87–0.96 ♀♀) times as long as mesotarsus. Metatibia 0.94 (0.97–1.03 ♂♂, 0.97–1.04 ♀♀) times as long as metatarsus. First pro-, meso-, and metatarsomere each almost equal to tarsomeres 2–4 combined. Length of protibia and protarsus combined 2.48 (2.32–2.48 ♂♂, 2.28–2.56 ♀♀) times as long as pronotum, length of mesotibia and mesotarsus combined 2.56 (2.54–2.74 ♂♂, 2.36–2.69 ♀♀) times as long as pronotum, while length of metatibia and metatarsus combined 3.77 (3.56–3.78 ♂♂, 3.50–3.75 ♀♀) times as long as pronotum.

Abdomen. Ventrites 2–7 with a very fine pubescence. Seventh ventrite with a pair of short ventral setae at its posterior margin. Male genital segment triangular, GSL: 0.81 mm, GSW: 0.49 mm.

Aedeagus. Median lobe of aedeagus slightly curved ventrally and elongate, narrowed apically, apical margin rounded (Figs 12–14), MLA: 0.73 mm, OML: 0.27 mm. Left paramere subtriangular, conchoid, about twice as long as wide, LPL: 0.26 mm; right paramere styliform, about three times as long as wide, distinctly shorter than the left one, RPL: 0.16 mm.

Female reproductive tract. Ovipositor (Figs 16, 17): with a broad laterotergite; basal gonocoxite 1 longer than apical gonocoxite 2, with three and four long trichoid setae apicoventrally, respectively (from left and right gonocoxites 1); gonocoxite 2 strongly curved, falciform in lateral aspect, with slightly rounded apex, with preapical setose organ circuloid ventrally, with four nematiform setae, laterodorsal surface with many marginal pit pegs (medially, on the lateroventral surface, the marginal pit pegs are located more apically). Female genital tract totally membranous (Fig. 15). Bursa copulatrix bulbous, without any expansion in

a bursal sacculus. Apically to the bursa copulatrix is the insertion point of common oviduct, which has a sharp curve to the right basally. Spermathecal insertion is in the helmonthoid sclerite, in the junction of common oviduct and bursa copulatrix. Spermatheca is markedly elongated and slender, widening distally. Spermathecal gland duct and spermathecal gland were not visualized. No secondary spermathecal gland observed.

Distribution. The species is widely distributed in caves from plateaus known as the N1N8 area in the northwestern part of the “Serra Norte de Carajás”, although a few specimens were also found in caves located southeast of the same plateaus at location “Serra Norte de Carajás”, state of Pará, Brazil (Figs 2, 4, 6).

***Coarazuphium kayapo* Pellegrini, Ferreira & Vieira, sp. nov.**

<http://zoobank.org/9280A871-017C-4D74-B1DA-46DF83182909>

Figs 3, 18–28

Type material. Holotype: BRAZIL: Pará, Serra Sul de Carajás, Cave S11B-0177, 6°20'21.4"S, 50°30'21.0"W, 641 m a.s.l., ♂, 24.IX.2018, Ativo Ambiental leg. (ISLA 75757).

Paratype. BRAZIL: Pará, Serra Sul de Carajás, Cave S11D-0111, 6°23'48.1"S, 50°20'27.3"W, 1 ♀, 17.VII–04.VIII.2010, Carste Company leg. (MZSP49198).

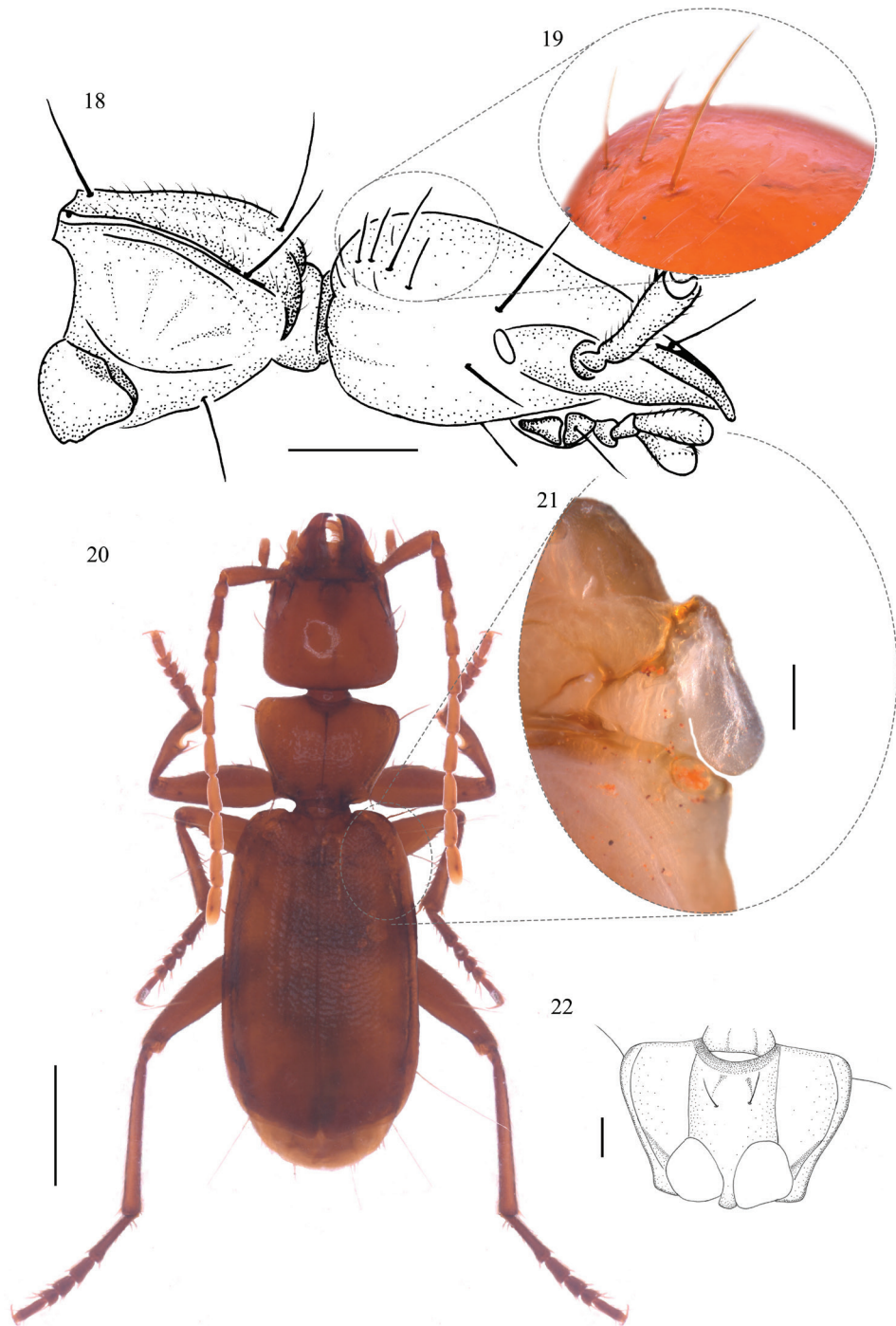
Etymology. The species name honors the Kayapó ethnic group, which is an important ethnic group of Brazilian indigenous people who live in the Amazon region. The natives do not designate themselves by this term, which was coined by neighboring groups to name them and which means “those who resemble monkeys”, which is probably due to a ritual during which the Kayapó men, dressed in monkey masks, perform short dances. The Kayapó refer themselves as the mebêngôkre, which means “the men of the hole/place of water”.

Differential diagnosis. All characteristics of *C. kayapo* sp. nov. are consistent with the description of the genus *Coarazuphium*. This species differs from all other members of the genus by the following combination of characters: elytral outline subparallel, elytra with maximum width in the posterior half, with a very slight preapical sinuosity; location of setigerous punctures on the head dorsally: one pair of anterior supraorbital, one pair of postocular and one pair of posterior supraorbital posteriad the eyes; three other pairs of setae, smaller in length, surrounding the latter setigerous punctures; head has a pubescence concentrated in the vertex margin, with long bristles; antennae long, about 0.76 times as long as body length; metafemur without a spine medially at the ventral side; median lobe of aedeagus about 2.77 as long as left paramere and 5.30 as long as right paramere.

Description. Size and proportions. OBL: 4.88 mm ♂, 4.96 mm ♀; EW: 1.61 mm ♂, 1.69 mm ♀; HW/PW: 0.93 ♂, 1.00 ♀.

Habitus. Body with uniform orange to brown color (Fig. 20).

Integument. Dorsally covered with short recumbent hairs.



Figures 18–22. *Coarazuphium kayapo* sp. nov., external morphology **18** head and prothorax, lateral view **19** a detail of fixed setae dorsally in the posterior portion of the head, lateral view **20** habitus, dorsal view **21** a detail of hind wings, dorsal view **22** prothorax, ventral view. Scale bars: 1.0 mm (**20**); 0.5 mm (**18**); 0.2 mm (**22**); 0.1 mm (**19, 21**).

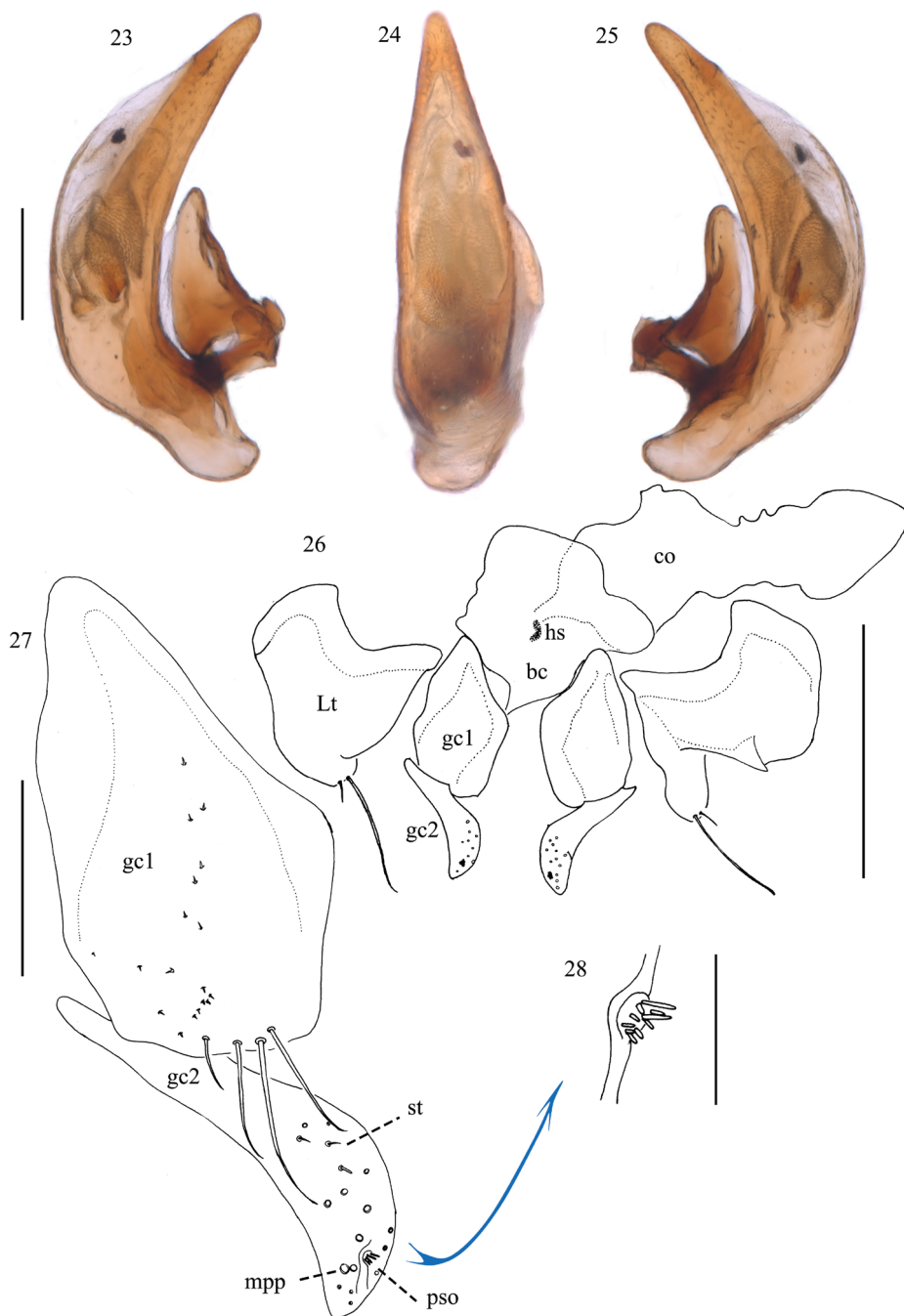
Head. Subtrapezoidal (Fig. 20), HW/HL: 0.91 ♂, 0.97 ♀. Head almost as wide as pronotum. Setigerous punctures on the head dorsally marginally to the vertex: one pair of anterior supraorbital above the eyes; one pair of postocular immediately behind the eyes, laterally; one pair of posterior supraorbital; three other pairs of setae, smaller in length, surrounding the latter setigerous punctures; among these smaller setae, there are two pairs of occipital setae; pubescence is concentrated on the vertex of the head, some of those bristles are almost of the size of medium-sized setae. Ventrally, the pubescence is sparse and the bristles are of varying size, located on the mentum, mentum suture and in the apical third of the post-gena. Associated with the post-gena, one pair of fixed setae is located more outwards apically, next to the submentum. There is also a pubescence irregular in size and position (Figs 18, 19). Eyes reduced, depigmented and flattened, situated laterally at the end of the genal sulcus, ommatidia are not visible at 50×. Antennae filiform and flagellar (Fig. 20), AL: 3.69 mm ♂, 3.59 ♀, AL/PL: 4.22 ♂, 4.03 ♀, A1L/A2–4L: 0.86 ♂, 0.88 ♀, of almost the same length in both genders. First antennomere (scape) with a long seta distally close to the apical portion, and a row of several semi-erect setae; 2nd one very short. Antennal segments 3–10 subequal and almost round in cross-section, except for the tip of the terminal antennomere, which is laterally flattened.

Prothorax. Pronotum trapezoidal, PL/PW: 0.72 ♂, 0.74 ♀ (Figs 18, 20). Maximum pronotum width closely behind the anterior margin, which is almost as wide as head. Anterior angle rounded. Posterior angle acute. Dorsal surface with two pairs of lateral marginal erect setae: one longer, close to the antero-lateral angles (about 0.43 times as long as pronotum), and the other shorter, close to the postero-lateral angles. Prosternum with a pair of submedial anterior setae (Fig. 22).

Pterothorax. Metasternum longer than wide. Metepisternum wider than long.

Elytra and hind wings. Elytra free (Fig. 20), EL/EW: 1.72 ♂, 1.67 ♀. Elytra sub-parallel, with maximum width in the posterior third, EW/PW: 1.33 ♂, 1.40 ♀. Elytral apex with a very slight sinuosity. Elytral chaetotaxy: no discal setae present; the umbilicate series of the 8th stria with seven large setae (about 0.43 times as long as elytra) on each elytron situated as follows: three close to the anterior angle, two marginal in the lateral posterior half, and two on the posterior margin. Hind wings are very reduced (Fig. 21), 0.275-mm long, HWL/EL: 0.10.

Legs. Profemur 1.06 (♂) and 1.03 (♀) times as long as mesofemur, and 0.71 (♂, ♀) times as long as metafemur, respectively. Protibia 0.99 (♂) and 1.17 (♀) times as long as mesotibia, and 0.69 (♂) and 0.73 (♀) times as long as metatibia, respectively. Protibia 1.18 (♂) and 1.35 (♀) times as long as protarsus, respectively. Mesotibia 0.99 (♂) and 0.90 (♀) times as long as mesotarsus, respectively. Metatibia 1.02 (♂) and 1.01 (♀) times as long as metatarsus. First pro-, meso-, and metatarsomere each almost equal to tarsomeres 2–4 combined. Length of protibia and protarsus combined 1.93 (♂) and 1.99 (♀) times as long as pronotum, length of mesotibia and mesotarsus combined 2.12 (♂) and 2.07 (♀) times as long as pronotum, while length of metatibia and metatarsus combined 3.02 (♂) and 3.10 (♀) times as long as pronotum, respectively.



Figures 23–28. *Coarazuphium kayapo* sp. nov., male and female genitalia **23** aedeagus, left lateral view **24** aedeagus, dorsal view **25** aedeagus, right lateral view **26** female reproductive tract, dorsal view **27** gonocoxite, dorsal view **28** preapical setose organ, dorsal view **bc** bursa copulatrix **co** common oviduct **gc1** gonocoxite 1 **gc2** gonocoxite 2 **hs** helminthoid sclerite **Lt** laterotergite **mpp** marginal pit **pegs** **psp** preapical setose organ **sp** spermatheca **spg** spermathecal gland **spgd** spermathecal gland duct **st** trichoid setae. Scale bars: 0.5 mm (**26**, **28**); 0.2 mm (**23–25**); 0.125 mm (**27**).

Abdomen. Ventrites 2–7 with a very fine pubescence. Seventh ventrite with a pair of small ventral setae at its posterior margin. Male genital segment oval, GSL: 0.96 mm, GSW: 0.56 mm.

Aedeagus. Median lobe of aedeagus slightly curved ventrally and elongate, narrowed apically, apical margin rounded (Figs 23–25), MLA: 0.82 mm, OML: 0.42 mm. Left paramere subtriangular, conchoid, about twice as long as wide, LPL: 0.30 mm; right paramere styliform, about three times as long as wide, distinctly shorter than the left one, RPL: 0.16 mm.

Female reproductive tract. Ovipositor (Figs 27, 28): with a broad laterotergite; basal gonocoxite 1 longer than apical gonocoxite 2, with three long trichoid setae apicoventrally, in addition to a smaller trichoid setae observed only on the right gonocoxite 1; gonocoxite 2 strongly curved, falciform in lateral aspect, with slightly rounded apex, with preapical setose organ circuloid ventrally, with four nematiform setae, laterodorsal surface with many marginal pit pegs medially (on the lateroventral surface, the marginal pit pegs are located more apically). Female genital tract totally membranous (Fig. 26). Bursa copulatrix bulbous, expanded in the bursal sacculus anterior to the common oviduct, which is curved to the right basally. Spermatheca, spermathecal gland duct, and spermathecal gland were broken and were not represented or visualized. No secondary spermathecal gland observed.

Distribution. This species is endemic to caves of the region known as “Serra Sul de Carajás” and is currently known to occur in two caves located approximately 10 km from each other (South Mountain, Flona de Carajás, Parauapebas, state of Pará, northern Brazil) (Figs 2, 4, 7).

***Coarazuphium xingu* Pellegrini, Ferreira & Vieira, sp. nov.**

<http://zoobank.org/B336E6F0-8012-47BF-9E43-C1815EE4B0CC>

Figs 29–38

Type material. Holotype: BRAZIL: Pará, São Félix do Xingu, Cave SFX-0057, 6°24'06.2"S, 51°54'08.1"W, ♂, 03.II.2018, Ativo Ambiental leg. (ISLA 75762).

Paratype: the same locality as for holotype, 1 ♀, 20.VII.2018, Ativo Ambiental leg. (ISLA 65430).

Etymology. The epithet *xingu* is given in designation to the type locality, where the two known specimens were collected. *Xingu* is an indigenous word that means “good and clean water” and names one of the main rivers in the region and an important indigenous reserve, the Parque Indigene do Xingu, currently the largest indigenous reserve in Brazil and one of the most important barriers to advanced agricultural development in the Amazon.

Differential diagnosis. All characteristics of *C. xingu* sp. nov. are consistent with the description of the genus *Coarazuphium*. This species differs from all others of the genus by the following combination of characters: elytral outline subparallel, elytra with maximum width in the posterior half, with a very slight subapical sinuosity; loca-

tion of setigerous punctures on the head dorsally: one anterior supraorbital and one postocular; antennae not very long, about 0.68 times as long as body length; metafemur without a spine medially at the ventral side.

Description. Size and proportions. OBL: 3.26 mm ♂, 3.19 mm ♀, EW: 1.09 mm ♂, 1.10 mm ♀, HW/PW: 1.07 ♂, 1.10 ♀.

Habitus. Body with uniform pale to dark brown color (Fig. 30).

Integument. Dorsally covered with short recumbent hairs.

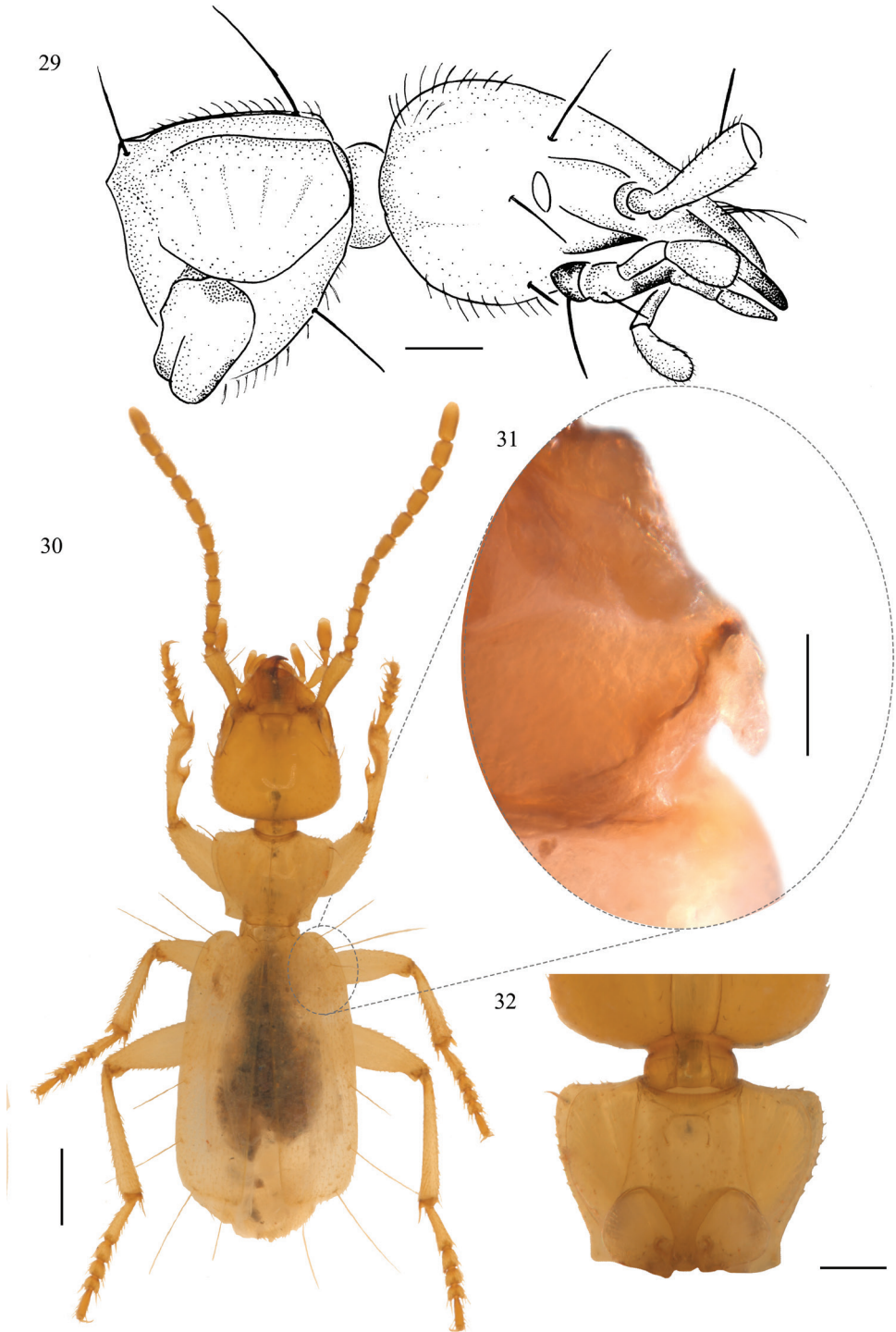
Head. Subtrapezoidal (Fig. 30), HW/HL: 0.91 ♂, 0.96 ♀. Head almost as wide as pronotum. Location of setigerous punctures on the head dorsally: one pair of anterior supraorbital above the eyes and one pair of postocular; head is covered with a fine pubescence more densely distributed on the vertex margin; ventrally are three pairs of setae on the post-gena located apically and a fine pubescence on the gula (Fig. 29). Eyes reduced, depigmented, and flattened, situated laterally at the end of the genal sulcus, ommatidia are not visible at 50× (Fig. 29). Antennae filiform and flagellar (Fig. 30), AL: 2.21 mm ♂, 2.11 mm ♀, AL/PL: 3.74 ♂, 3.67 ♀, A1L/A2–4L: 0.76 ♂, 0.75 ♀. First antennomere (scape) with a long seta distally close to the apical portion, and a row of several semi-erect setae; 2nd one very short. Antennal segments 3–10 subequal, rectangular, and almost round in cross-section, except for the tip of the terminal antennomere, which is laterally flattened.

Prothorax. Pronotum trapezoidal, PL/PW: 0.75 ♂, 0.79 ♀ (Figs 29, 30). Maximum pronotum width closely behind the anterior margin, which is almost as wide as head. Anterior angle rounded. Posterior angle acute. Dorsal surface with two pairs of lateral marginal erect setae: one close to the antero-lateral angles, and the other shorter, close to the postero-lateral angles. Prosternum with a pair of sub-medial setae (Fig. 32).

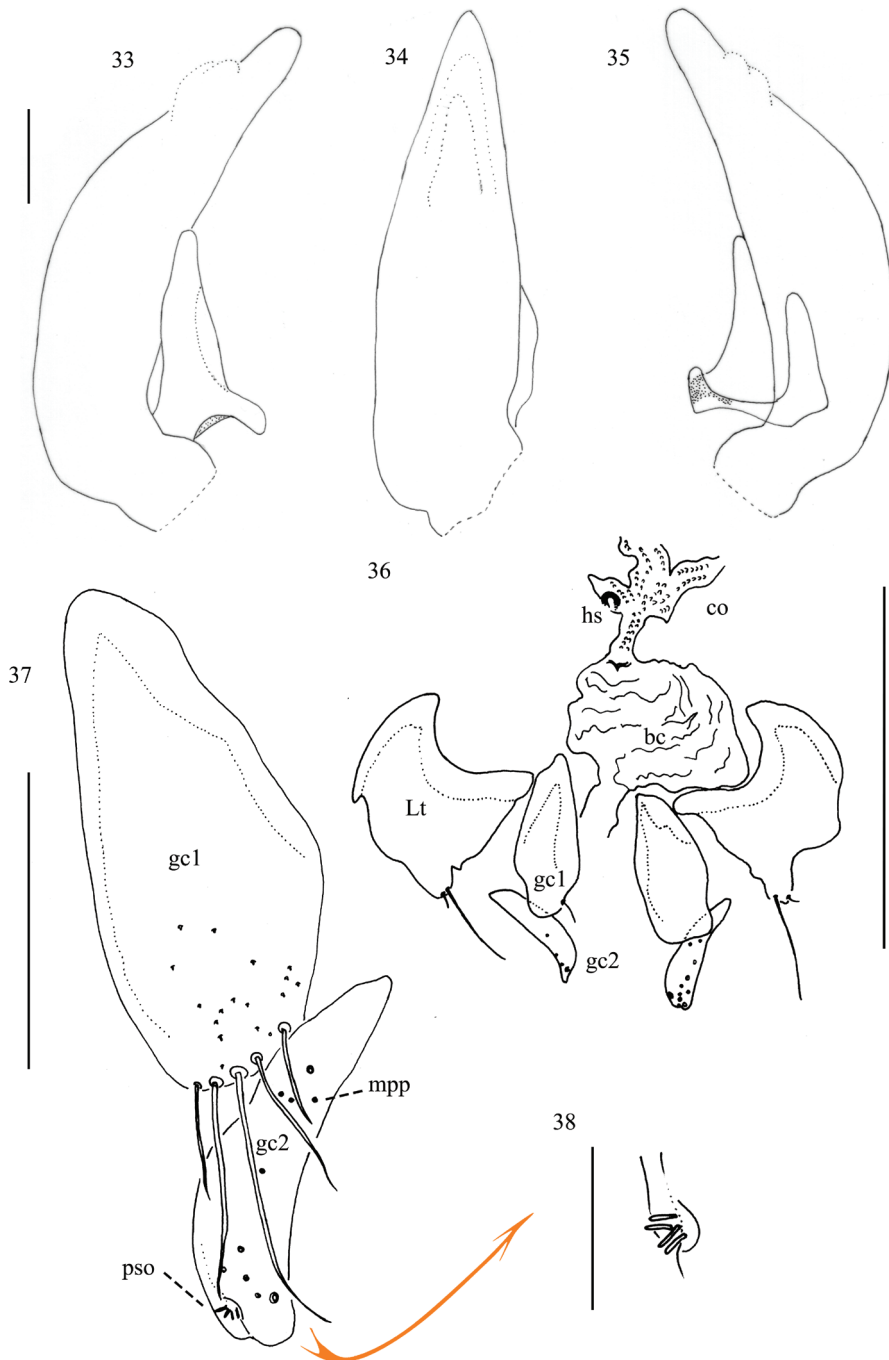
Pterothorax. Metasternum longer than wide. Metepisternum wider than long.

Elytra and hind wings. Elytra free (Fig. 30), EL/EW: 1.60 ♂, 1.62 ♀. Elytral outline subparallel, maximum elytral width in the posterior half, EW/PW: 1.39 ♂, 1.50 ♀. Subapical elytral sinuosity very slight. Elytral chaetotaxy: no discal setae present; the umbilicate series of the 8th stria with seven large setae (about 0.58 times as long as elytra) on each elytron: three close to the anterior angle, two marginal in the lateral posterior half, and two on the posterior margin. Hind wings very reduced (Fig. 31), 0.10-mm long, HWL/EL: 0.06 ♂.

Legs. Profemur 1.21 (♂) and 1.12 (♀) times as long as mesofemur, and 0.84 (♂) and 0.76 (♀) times as long as metafemur, respectively. Protibia 1.23 (♂) and 1.05 (♀) times as long as mesotibia, and 0.79 (♂) and 0.75 (♀) times as long as metatibia, respectively. Protibia 1.28 (♂) and 1.20 (♀) times as long as protarsus, mesotibia 0.81 (♂) and 0.97 (♀) times as long as mesotarsus, and metatibia 0.93 (♂) and 1.01 (♀) times as long as metatarsus, respectively. First pro-, meso-, and metatarsomere each almost equal to tarsomeres 2–4 combined. Length of protibia and protarsus combined 2.04 (♂) and 2.01 (♀) times as long as pronotum, length of mesotibia and mesotarsus 2.09 (♂) and 2.11 (♀) times as long as pronotum, while length of metatibia and metatarsus 2.99 (♂) and 2.91 (♀) times as long as pronotum, respectively.



Figures 29–32. *Coarazuphium xingu* sp. nov., external morphology **29** head and prothorax, lateral view **30** habitus, dorsal view **31** a detail on hind wings, dorsal view **32** prothorax, ventral view. Scale bars: 0.5 mm (**30**), 0.2 mm (**29, 32**); 0.1 mm (**31**).



Figures 33–38. *Coarazuphium xingu* sp. nov., male and female genitalia **33** aedeagus, left lateral view **34** aedeagus, dorsal view **35** aedeagus, right lateral view **36** female reproductive tract, dorsal view **37** gonocoxite, dorsal view **38** preapical setose organ, dorsal view **bc** bursa copulatrix **co** common oviduct **gc1** gonocoxite 1 **gc2** gonocoxite 2 **hs** helminthoid sclerite **Lt** laterotergite **mpp** marginal pit pegs **pso** preapical setose organ. Scale bars: 0.5 mm (**36, 38**); 0.125 mm (**37**); 0.1 mm (**33–35**).

Abdomen. Ventrites 2–7 with a very fine pubescence. Seventh ventrite with a pair of small ventral setae at its posterior margin. Male genital segment triangular, GSL: 0.65 mm, GSW: 0.38 mm.

Aedeagus. Median lobe of aedeagus slightly curved ventrally and elongate, narrowed apically, apical margin rounded (Figs 33–35), MLA: 0.58 mm, OML: 0.15 mm. Left paramere subtriangular, conchoid, about twice as long as wide, LPL: 0.21 mm; right paramere styliform, about three times as long as wide, distinctly shorter than the left one, RPL: 0.15 mm.

Female reproductive tract. Ovipositor (Figs 37, 38): with a broad laterotergite; basal gonocoxite 1 longer than apical gonocoxite 2, with two small and three long trichoid setae apicoventrally; gonocoxite 2 strongly curved, falciform in lateral aspect, with notched apex, with preapical setose organ circuloid ventrally, with four nemati-form setae, laterodorsal surface with many marginal pit pegs medially (on the lateroventral surface, the marginal pit pegs are located more apically). Female genital tract totally membranous (Fig. 36). Bursa copulatrix bulbous, expanded in the bursal sacculus anteriorly to the insertion point of common oviduct, which is curved basally and partially broken. Spermatheca, spermathecal gland duct, and spermathecal gland were broken and were not represented or visualized. No secondary spermathecal gland observed.

Distribution. The species was found in a single cave located in the municipality of São Felix do Xingu, state of Pará, Brazil (Figs 2, 4, 5).

Comparative diagnosis

The *Coarazuphium* species that occur in the Carajás region are morphologically similar, those are likely each other's closest living relatives, and are distributed in a small geographic range. From the six known species, two stand out: *C. spinifemur* and *C. xingu* sp. nov., which are the smallest *Coarazuphium* species. They both possess shorter legs and antennae when compared to the remaining species. The main characteristic that distinguishes *C. xingu* sp. nov. from *C. spinifemur* is the presence of a femoral spine in the latter species. In addition to the general proportions of the body (i.e., less elongated antennae and legs), other combination of characters – such as the existence of only two dorsal setigerous punctures on the head, head quadrangular and elytra with almost parallel sides, with the apical margin only slightly sinuated – also makes *C. xingu* sp. nov. unique morphologically.

With an overall body form very similar to that of the other two species from the Carajás region (*C. tapiaguassu* and *C. amazonicum*), the main characteristic that distinguishes *C. xikrin* sp. nov. and *C. kayapo* sp. nov. from the above mentioned two species is the number of setigerous punctures dorsally on the head. The two former species have only two pairs of fixed setae dorsally on the head: one pair of anterior supraorbital and one pair of postocular. Besides those setae, *C. xikrin* sp. nov. also bears one pair of posterior supraorbital setae. *Coarazuphium kayapo* sp. nov. possesses, in addition to the three pairs of setae mentioned, one pair of posterior supernumerary setae and two pairs of occipital setae. *Coarazuphium xikrin* sp. nov. can be distinguished from all other *Coarazuphium* species by possessing the described

setae posteriorly on the head, quadrangular head, elytra with almost parallel sides, with the apical margin truncate. *Coarazuphium kayapo* sp. nov. can be distinguished from the other *Coarazuphium* species by possessing the described setae posteriorly on the head, quadrangular head, elytra with almost parallel sides, with the apical margin only slightly sinuated.

Key for identification of adults of species of the genus *Coarazuphium* (modified after Pellegrini et al. 2021)

- 1 Elytra with apical margin truncate, not sinuate (Pellegrini and Ferreira 2011: 49, Fig. 2A) **2**
- Elytra with apical margin sinuate (Godoy and Vanin 1990: 796, Fig. 1) or with a slight apical sinuosity (Pellegrini et al. 2020: 291, Fig. 5) **9**
- 2(1) Head dorsally bearing two pairs of setae: one pair of anterior supraorbital and one pair of postocular (Pellegrini and Ferreira 2017: 556, Fig. 5) **3**
- Head dorsally bearing three or more pairs of setae, rarely two pairs. If only two setae are present, the postocular seta is absent **5**
- 3(2) Metafemur with a spine medially at the ventral side (Pellegrini and Ferreira 2017: 556, Fig. 4), antennae short, about 0.68 times as long as total body length ***C. spinifemur* Pellegrini & Ferreira, 2017**
- Metafemur without a spine medially at the ventral side, antennae long, reaching metafemur insertion **4**
- 4(3') Aedeagus very long and slender, about 2.89 times as long as left paramere (Pellegrini and Ferreira 2011: 49, Figs 2D–F) ***C. tapiaguassu* Pellegrini & Ferreira, 2011**
- Aedeagus shorter, about 2.60 times as long as left paramere (Pellegrini and Ferreira 2017: 557, Figs 6C–E) ***C. amazonicum* Pellegrini & Ferreira, 2017**
- 5(2') Head dorsally bearing only two pairs of setae: one pair of anterior supraorbital and one pair of posterior supraorbital (Bená and Vanin 2014: 291, Fig. 5) ... ***C. ricardo* Bená & Vanin, 2014**
- Head dorsally with three or more pairs of setae: at least one pair of anterior supraorbital, one pair of postocular and one pair of posterior supraorbital .. **6**
- 6 Head dorsally with three pairs of setae (Pellegrini et al. 2021: 6, Fig. 8) ***C. auleri* Pellegrini & Vieira, 2021**
- Head dorsally with more than three pairs of setae **7**
- 7(6') Five pairs of setae on the head dorsally: occipital and posterior supraorbital setae placed beyond anterior supraorbital, postocular and posterior supernumerary setae (Ball and Shpeley 2013: 30, Fig. 4A).... ***C. whiteheadi* Ball & Shpeley, 2013**
- Four pairs of setae on the head dorsally **8**
- 8(7') Besides anterior supraorbital, postocular and posterior supernumerary setae, head dorsally bearing one pair of posterior supraorbital setae, located more anterior and lateral than posterior supernumerary setae (Pellegrini et al. 2020: 297, Fig. 22) ***C. pains* Álvares & Ferreira, 2002**

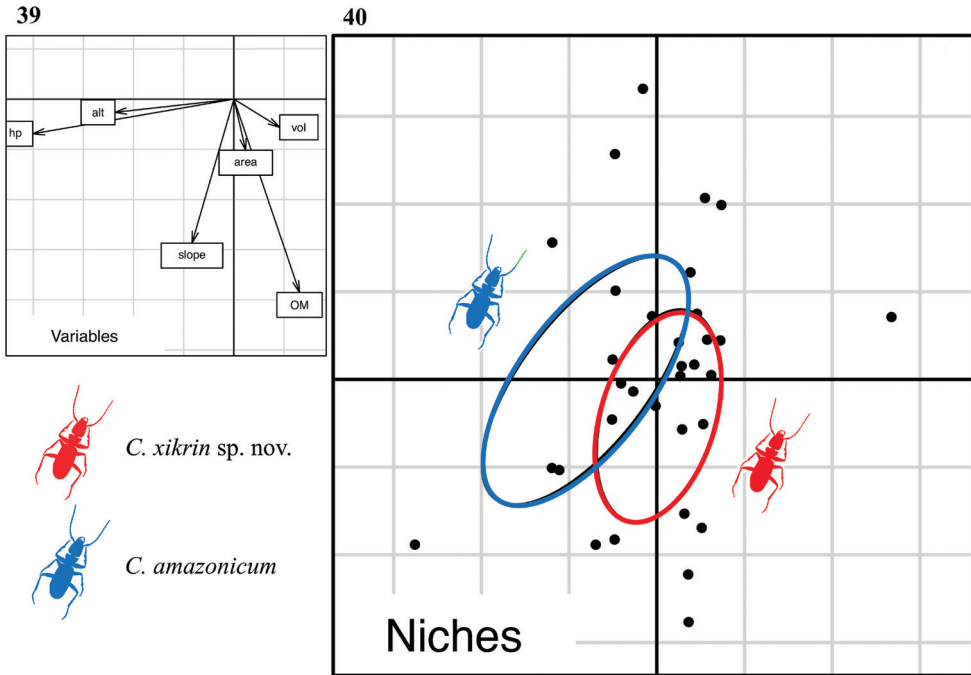
- Besides anterior supraorbital, postocular and posterior supernumerary setae, head dorsally bearing one pair of occipital setae, located more posterior and medially than posterior supernumerary setae (Fig. 8) ***C. xikrin* sp. nov.**
- 9(1') Head dorsally bearing two to three pairs of setae, anterior supraorbital and postocular setae always present..... **10**
- Head dorsally bearing four to five pairs of setae, anterior supraorbital, postocular, posterior supernumerary and occipital setae always present **13**
- 10(9') Head dorsally bearing only two pairs of setae: one pair of anterior supraorbital and one pair of postocular (Fig. 29) ***C. xingu* sp. nov.**
- Head dorsally bearing three pairs of setae..... **11**
- 11(10) Head elongate, HW/HL about 0.60.....
..... ***C. cessaima* Gnaspini, Vanin & Godoy, 1998**
- Head subquadrangular, HW/HL 0.95 **12**
- 12(11') Left paramere styliform (Godoy and Vanin 1990: 798, Fig. 2), elytra with one pair of short setae behind scutellum and two pairs of discal setae (Godoy and Vanin 1990: 798, Fig. 1) ***C. tessai* (Godoy & Vanin, 1990)**
- Left paramere broad, conchoid (Pellegrini et al. 2022: 564, Fig. 11), elytra without discal setae or any setae behind scutellum
..... ***C. bambui* Pellegrini & Vieira, 2022**
- 13(9') Head dorsally with two pairs of occipital setae (Pellegrini and Ferreira 2014: 529, Fig. 2B) **14**
- Head dorsally with one pair of occipital setae..... **16**
- 14(13) Head dorsally having a pubescence (Fig. 18), with posterior medium-sized setae anterior and lateral to posterior supernumerary setae ***C. kayapo* sp. nov.**
- Head dorsally glabrous, except for fixed setae **15**
- 15(14) Elytra with a slight apical sinuosity (Pellegrini and Ferreira 2014: 537, Figs 12A, C), head dorsally without protuberances
..... ***C. formoso* Pellegrini & Ferreira, 2011**
- Elytra with a pronounced apical sinuosity, head dorsally with two protuberances (Pellegrini and Ferreira 2014: 537, Figs 12B, D).....
..... ***C. caatinga* Pellegrini & Ferreira, 2014**
- 16(13') Head dorsally bearing one pair of posterior supernumerary setae (Pellegrini et al. 2020: 293, Fig. 6) ***C. lundi* Pellegrini, Ferreira & Vieira, 2020**
- Head dorsally without posterior supernumerary setae
..... ***C. bezerra* Gnaspini, Vanin & Godoy, 1998**

Habitat preferences and niche overlap

Comparing niches from two *Coarazuphium* species, *C. amazonicum* and *C. xikrin* sp. nov., revealed that the latter species is more tolerant to the average environmental conditions available in the caves located at Serra Norte de Carajás (Table 1, Figs 39, 40). *Coarazuphium amazonicum*, in turn, is preferentially associated to caves with wider horizontal projection.

Table I. OMI analysis results.

	Inertia	OMI	Tol	Rtol	p-value
<i>C. amazonicum</i>	6.257	0.662	1.422	4.174	0.05
<i>C. xikrin</i> sp. nov.	4.974	0.176	1.442	3.356	0.05
OMI mean					0.05



Figures 39–40. Results of the outlying mean index (OMI) for *C. xikrin* sp. nov. and *C. amazonicum* **39** principal component analysis (PCA) of the environmental variables showing the covariation of variables in relation to the cave and the niche representation **40** representation of the occupied niche for the analyzed species in relation to the environmental variables. The black dots represent the sampling points, corresponding to each cave **alt** altitude **area** the area of the cave floor **hp** horizontal projection **OM** diversity of organic matter resources available **slope** the slope of the cave floor **vol** cave volume

Discussion

Niche overlap patterns of two co-existing species

Ecological theory predicts that high competition rates reduce a species' realized niche, and this competition is often intensified in cave environments (Culver 1970). The presence of related species in an environment with low-resource availability, such as caves, intensifies intra- and interspecific competition pressure, especially among top predator species (Mammola et al. 2016). On small scales, co-existing species tend to evolve divergent habitat preferences that allow their coexistence in the cave's harsh habitat (Mammola et al. 2016; Martins and Ferreira 2020).

We found evidence for niche differentiation between *C. xikrin* sp. nov. and *C. amazonicum*. *Coarazuphium xikrin* sp. nov. is apparently more tolerant to the average conditions available in the caves of the Carajás region, while *C. amazonicum* is preferentially associated with larger caves. It is well known by the speleological community that bigger caves shelter a higher number of species. The species-area relationship has been empirically tested and confirmed in a variety of taxonomic groups (Schneider and Culver 2004; Souza-Silva and Ferreira 2011; Ferreira and Pellegrini 2019; Souza-Silva et al. 2020), and larger caves are generally associated with higher availability of food resources and with higher environmental heterogeneity. Hence, bigger caves typically possess more niches available for colonization.

A hotspot for troglobitic beetles in South America

Considering the current distribution of *Coarazuphium* species, the iron ore caves of the southeastern portion of the state of Pará, especially the Carajás region, shelter the highest known diversity of the genus. So far, six *Coarazuphium* species have been described from this region, and this richness corresponds to approximately 40% of the known species. Most *Coarazuphium* species, especially those associated with limestone caves, are infrequently collected and endemic (for several species only a few specimens are known). However, in the Carajás region, certain species are abundant and distributed in dozens of caves, including cases of sympatry, as observed for *C. amazonicum* and *C. xikrin* sp. nov. in the Serra Norte area, and for *C. tapiaguassu* and *C. spinifemur* in the Serra Leste area (Fig. 4).

The Carajás region corresponds to one of the most important mineral reserves in Brazil, and the current protection of the caves by the Brazilian government represents a major environmental obstacle to overexploitation of such mineral resources. Therefore, the maintenance of legal provisions that ensure the preservation of caves is crucial for the conservation of Brazilian subterranean biodiversity. This is even more important for the most relevant caves regarding physical and biotic aspects, especially in this region that represents a hotspot of cave beetles. In addition to the six *Coarazuphium* species, several other troglobitic beetle taxa are known to occur in caves in the region, including the following: *Copelatus cessaima* Caetano, Bená & Vanin, 2013 (Dytiscidae), *Ardistomis ferreirai* Balkenohl, Pellegrini & Zampaulo, 2018 (Clivinini, Carabidae), and *Metopioxys carajas* Asenjo, 2019 (Pselaphinae, Staphylinidae). Furthermore, several other troglobitic species from different invertebrate groups (mostly arthropods) also exist in Carajás, including spiders – Oonopidae (many species), Caponiidae (*Carajas paraua* Brescovit & Sánchez-Ruiz, 2016), Gnaphosidae (*Pracymbionna carajas* Rodrigues, Cizauskas & Rheims, 2018), Tetrablemmidae (*Matta* sp.), and Ochyroceratidae (*Speocera* spp., *Ochyrocera* spp.); tailless whip scorpions – Charinidae (*Charinus ferreus* Giupponi & Miranda, 2016); harvestmen – Escadabiidae (many species); pseudoscorpions – Bochicidae, Chthoniidae, and Ideoroncidae (many species); millipedes – Glomeridesmidae (*Glomeridesmus spelaeus* Iniesta, Ferreira & Wesener, 2012), Pyrgodesmidae (many species), and Pseudonannolenidae (*Pseudonannolene* spp.); springtails – Paronellidae (*Trogolaphysa* sp., *Cyphoderus* sp.), Entomobryidae (*Pseudosinella* sp.), and Sminthuridae

(*Pararrhopalites* sp.); woodlice – Scleropactidae (*Circoniscus* spp.) and Calabozoidae; amphipods – Bogidiellidae (*Bogidiella* sp.); and flatworms – Prorhynchidae (*Geocentrophora* sp.) (Brescovit et al. 2021). Bento et al. (2021) discussed about the Brazilian areas of great biospeleological relevance. Amongst the 10 regions mentioned in this work, the Carajás region stood out as the second in absolute number of troglobitic species. The area with the highest number of cave-restricted species comprised the Atlantic Forest as a whole, and this high number is certainly a result of the large extension of this domain, in comparison with the other more spatially restricted areas presented. Furthermore, it should be noted that the Carajás region also possesses a very unique troglobitic fauna, with species belonging to groups that only occur in this region (Ferreira et al. 2018).

The Xingu River basin region represents a large corridor of protected areas and its protection remains one of the most effective barriers against deforestation in the Brazilian Amazon. However, studies carried out by non-governmental associations reveal a significant increase in deforestation in the region in the last few years. Between 2018 and 2020, 513,500 hectares were deforested in the Xingu basin. Instead of implementing measures to protect the Xingu Reserve, the Brazilian government has promoted a scenario of total impunity through rhetoric favorable to the unconstitutional reduction of indigenous lands and the legalization of destructive activities, such as mining, in addition to weakening oversight (Instituto Socioambiental – ISA 2020; MapBiomias 2021). Therefore, despite the high biological relevance of those areas, which shelter an exceptionally high set of unique subterranean fauna, all the cave-restricted species are more threatened than ever.

Acknowledgements

We thank Sônia Casari, Ana Vásquez, and Daniela Bená, who help in gathering a part of the type material that was deposited in the MZSP. We also thank Xavier Prous, Matheus Simões, Thadeu Pietrobon, and the entire Vale's Speleology Department for gathering information on caves and granting access to its speleology database. This work was supported by Vale S.A. and Fundação de Amparo à Pesquisa do Estado de Minas Gerais (FAPEMIG), project number: RDP 00092-18 and by a scholarship provided to RLF (CNPq no. 308334/2018-3). We are also grateful to Borislav Guéorguiev, Antonio Gomez, Thierry Deuve and the subject editor Srećko Ćurčić for their suggestions in the review process that certainly improved the manuscript.

References

- Álvares ESS, Ferreira RL (2002) *Coarazuphium pains*, a new species of troglobitic beetle from Brazil (Coleoptera: Carabidae: Zuphiini). *Lundiana* 3: 41–43.
- Ball GE, Shpeley D (2013) Western Hemisphere Zuphiini: descriptions of *Coarazuphium whiteheadi*, new species, and *Zuphioides*, new genus, and classification of the genera (Coleoptera, Carabidae). *ZooKeys* 315: 17–54. <https://doi.org/10.3897/zookeys.315.5293>

- Barlas E, Yamaç E (2019) Cave dwelling bat species and their cave preferences in North-west of Central Anatolia. *Pakistan Journal of Zoology* 51(6): 2141–2151. <https://doi.org/10.17582/journal.pjz/2019.51.6.2141.2151>
- Bená DC, Vanin SA (2014) A new troglobitic species of *Coarazuphium* Gnaspini, Vanin & Godoy (Coleoptera, Carabidae, Zuphiini) from a cave in Paraná State, Southern Brazil. *Zootaxa* 3779(2): 288–296. <https://doi.org/10.11646/zootaxa.3779.2.9>
- Bento DM, Souza-Silva M, Vasconcellos A, Bellini BC, Prous X, Ferreira RL (2021) Subterranean “oasis” in the Brazilian semiarid region: neglected sources of biodiversity. *Biodiversity and Conservation* 30(13): 3837–3857. <https://doi.org/10.1007/s10531-021-02277-6>
- Brasil (2008) Decreto Federal No 6.640, de 07 de novembro de 2008. Relevância de cavernas. Diário Oficial da República Federativa do Brasil, Brasília. www.planalto.gov.br/ccivil_03/_ato2007-2010/2008/decreto/d6640.htm
- Brasil (2017) Ministério do Meio Ambiente – Instrução Normativa No 2 de 30 de Agosto de 2017. Define a metodologia para classificação do grau de relevância das cavidades naturais subterrâneas. Diário Oficial da República Federativa do Brasil, Brasília. https://www.in.gov.br/materia/-/asset_publisher/Kujrw0TZC2Mb/content/id/19272154/do1-2017-09-01-instrucao-normativa-n-2-de-30-de-agosto-de-2017-19272042
- Brescovit AD, Zampaulo RDA, Cizauskas I (2021) The first two blind troglobitic spiders of the genus *Ochyrocera* from caves in Floresta Nacional de Carajás, state of Pará, Brazil (Araneae, Ochyroceratidae). *ZooKeys* 1031: 143–159. <https://doi.org/10.3897/zookeys.1031.62181>
- Campos JF, Castilho A (2012) Uma visão geográfica da Região da Flona de Carajás. In: Martins FD, Castilho AF, Campos JF, Hatano FM, Rolim SG (Eds) Floresta Nacional de Carajás: estudos sobre vertebrados terrestres. Nitro Imagens, São Paulo, 28–63.
- CECAV (2021) Cadastro Nacional de Informações Espeleológicas (CANIE). Instituto Chico Mendes de Conservação da Biodiversidade (ICMBio), Brasília. <https://www.icmbio.gov.br/cecav/canie.html>
- Culver DC (1970) Analysis of simple cave communities: niche separation and species packing. *Ecology* 51(6): 949–958. <https://doi.org/10.2307/1933622>
- Dayan T, Simberloff D (2005) Ecological and community-wide character displacement: the next generation. *Ecology Letters* 8(8): 875–894. <https://doi.org/10.1111/j.1461-0248.2005.00791.x>
- Deuve T (1993) L'abdomen et les genitalia des femelles de Coléoptères Adephaga. *Mémoires du Muséum national d'histoire naturelle, Série A, Zoologie* 155: 1–184.
- Dolédec S, Chessel D, Gimaret-Carpentier C (2000) Niche separation in community analysis: a new method. *Ecology* 81(10): 2914–2927. [https://doi.org/10.1890/0012-9658\(2000\)081\[2914:NSICAA\]2.0.CO;2](https://doi.org/10.1890/0012-9658(2000)081[2914:NSICAA]2.0.CO;2)
- Dray S, Dufour A (2007) The ade4 package: implementing the duality diagram for ecologists. *Journal of Statistical Software* 22(4): 1–20. <https://doi.org/10.18637/jss.v022.i04>
- Ferreira ATR, Lamarão CN (2013) Geologia, petrografia e geoquímica das rochas vulcânicas Uatumã na área sul de São Félix do Xingu (PA), Província Carajás. *Brazilian Journal of Geology* 43(1): 152–167. <https://doi.org/10.5327/Z2317-48892013000100013>
- Ferreira RL, Pellegrini TG (2019) Species-area model predicting diversity loss in an artificially flooded cave in Brazil. *International Journal of Speleology* 48: 155–165. <https://doi.org/10.5038/1827-806X.48.2.2244>

- Ferreira RL, Oliveira MPAD, Silva MS (2018) Subterranean biodiversity in ferruginous landscapes. In: Moldovan OT, Kováč L, Halse S (Eds) Cave Ecology. Springer, Cham, 435–447. https://doi.org/10.1007/978-3-319-98852-8_21
- Gnaspini P, Vanin SA, Godoy NM (1998) A new genus of troglobitic carabid beetles from Brazil (Coleoptera, Carabidae, Zuphiini). *Papéis Avulsos de Zoologia* 40: 297–309.
- Godoy NM, Vanin SA (1990) *Parazuphium tessai*, sp. n., a new cavernicolous beetle from Bahia, Brazil (Coleoptera, Carabidae, Zuphiini). *Revista Brasileira de Entomologia* 34: 795–799.
- Instituto Socioambiental – ISA (2020) Xingu under Bolsonaro: Xingu River basin deforestation assessment (2018–2020). São Paulo, Brazil, 48 pp. https://www.socioambiental.org/sites/blog.socioambiental.org/files/nsa/arquivos/sx_3a_en_af02.pdf
- Jaffé R, Prous X, Zampaulo R, Giannini TC, Imperatriz-Fonseca VL, Maurity C, Oliveira G, Brandi IV, Siqueira JO (2016) Reconciling mining with the conservation of cave biodiversity: a quantitative baseline to help establish conservation priorities. *PLoS ONE* 11(12): e0168348. <https://doi.org/10.1371/journal.pone.0168348>
- Jaffé R, Prous X, Calux A, Gastauer M, Nicacio G, Zampaulo R, Souza-Filho PWM, Oliveira G, Brandi IV, Siqueira JO (2018) Conserving relics from ancient underground worlds: assessing the influence of cave and landscape features on obligate iron cave dwellers from the Eastern Amazon. *PeerJ* 6: e4531. <https://doi.org/10.7717/peerj.4531>
- Liebherr JK (2015) The *Mecyclothorax* beetles (Coleoptera, Carabidae, Moriomorphini) of Haleakala-, Maui: keystone of a hyperdiverse Hawaiian radiation. *ZooKeys* 544: 1–407. <https://doi.org/10.3897/zookeys.544.6074>
- Liebherr JK, Will KM (1998) Inferring phylogenetic relationships within Carabidae (Insecta, Coleoptera) from characters of the female reproductive tract. In: Ball GE, Casale A, Vigna Taglianti A (Eds) Phylogeny and Classification of Caraboidea (Coleoptera: Adephaga), XX International Congress of Entomology (1996, Firenze, Italy). Museo Regionale di Scienze Naturali di Torino, Turin, 107–170.
- Mammola S, Piano E, Isaia M (2016) Step back! Niche dynamics in cave-dwelling predators. *Acta Oecologica* 75: 35–42. <https://doi.org/10.1016/j.actao.2016.06.011>
- MapBiomias (2021) Annual Report on Deforestation in Brazil 2020. São Paulo, Brazil, 93 pp. https://s3.amazonaws.com/alerta.mapbiomas.org/rad2020/RAD2021_-
- Martins FD, Esteves E, Reis ML, Costa FG (2012) Ações para conservação. In: Martins FD, Castilho AF, Campos JF, Hatano FM, Rolim S (Eds) Floresta Nacional de Carajás: estudos sobre vertebrados terrestres. Nitro Imagens, São Paulo, 198–229.
- Martins VM, Ferreira RL (2020) Limiting similarity in subterranean ecosystems: a case of niche differentiation in Elmidae (Coleoptera) from epigeal and hypogean environments. *Hydrobiologia* 847(2): 593–604. <https://doi.org/10.1007/s10750-019-04123-x>
- Mayfield MM, Levine JM (2010) Opposing effects of competitive exclusion on the phylogenetic structure of communities. *Ecology Letters* 13(9): 1085–1093. <https://doi.org/10.1111/j.1461-0248.2010.01509.x>
- Mertens B, Pocard-Chapuis R, Piketty MG, Lacques AE, Venturieri A (2002) Crossing spatial analyses and livestock economics to understand deforestation processes in the Brazilian Amazon: the case of Sao Felix do Xingu in South Para. *Agricultural Economics* 27: 269–294. <https://doi.org/10.1111/j.1574-0862.2002.tb00121.x>

- Oliveira G, Chen JM, Mataveli GAV, Chaves MED, Seixas HT, Cardozo FS, Shimabukuro YE, He L, Stark SC, Santos CAC (2020) Rapid recent deforestation incursion in a vulnerable indigenous land in the Brazilian Amazon and fire-driven emissions of fine particulate aerosol pollutants. *Forests* 11(8): e829. <https://doi.org/10.3390/f11080829>
- Pellegrini TG, Ferreira RL (2011) *Coarazuphium tapiaguassu* (Coleoptera: Carabidae: Zuphiini), a new Brazilian troglobitic beetle with ultrastructural analysis and ecological considerations. *Zootaxa* 3116(1): 47–58. <https://doi.org/10.11646/zootaxa.3116.1.3>
- Pellegrini TG, Ferreira RL (2014) Ultrastructural analysis in *Coarazuphium caatinga* (Coleoptera: Carabidae: Zuphiini), a new Brazilian troglobitic beetle. *Zootaxa* 3765(6): 526–540. <https://doi.org/10.11646/zootaxa.3765.6.2>
- Pellegrini TG, Ferreira RL (2017) Two new troglobitic *Coarazuphium* Gnaspini, Godoy & Vannin, 1998 species of ground beetles from iron ore Brazilian caves (Coleoptera: Carabidae: Zuphiini). *Zootaxa* 4306(4): 551–566. <https://doi.org/10.11646/zootaxa.4306.4.6>
- Pellegrini TG, Bichuette ML, Vieira L (2021) *Coarazuphium auleri* sp. n. (Carabidae: Zuphiini), a new troglobitic ground-beetle in Central-Western Brazil. *Studies on Neotropical Fauna and Environment*, 1–11. <https://doi.org/10.1080/01650521.2021.2010975>
- Pellegrini TG, Bichuette ML, Vieira L (2022) *Coarazuphium bambui* (Carabidae: Zuphiini), a new cave-dwelling beetle from the threatened region of Serra do Ramalho, Brazil. *Zootaxa* 5129(4): 557–568. <https://doi.org/10.11646/ZOOTAXA.5129.4.5>
- Pellegrini TG, Ferreira RL, Zampaulo RA, Vieira L (2020) *Coarazuphium lundi* (Carabidae: Zuphiini), a new Brazilian troglobitic beetle, with the designation of a neotype for *C. pains* Álvares Ferreira, 2002. *Zootaxa* 4878(2): 287–304. <https://doi.org/10.11646/zootaxa.4878.2.4>
- R Core Team (2019) R: A Language and Environment for Statistical Computing. R Foundation for Statistical Computing, Vienna. <https://www.R-project.org/>
- Rizzo R, Garcia AS, Vilela VMFN, Ballester MVR, Neill C, Victoria DC, Rocha HR, Coe MT (2020) Land use changes in Southeastern Amazon and trends in rainfall and water yield of the Xingu River during 1976–2015. *Climatic Change* 162(3): 1419–1436. <https://doi.org/10.1007/s10584-020-02736-z>
- Rolim SG, Couto HTZ, Jesus RM, França JT (2006) Modelos volumétricos para a Floresta Nacional do Tapirapé-Aquirí, Serra dos Carajás (PA). *Acta Amazonica* 36(1): 107–114. <https://doi.org/10.1590/S0044-59672006000100013>
- Schneider K, Culver DC (2004) Estimating subterranean species richness using intensive sampling and rarefaction curves in a high density cave region in West Virginia. *Journal of Cave and Karst Studies* 66(2): 39–45.
- Souza-Filho PWM, Souza EB, Silva Júnior RO, Nascimento Jr WR, Mendonça BRV, Guimarães JTF, Dall’Agnol R, Siqueira JO (2016) Four decades of land-cover, land-use and hydroclimatology changes in the Itacaiúnas River watershed, southeastern Amazon. *Journal of Environmental Management* 167: 175–184. <https://doi.org/10.1016/j.jenvman.2015.11.039>
- Souza-Silva M, Martins RP, Ferreira RL (2011) Cave lithology determining the structure of the invertebrate communities in the Brazilian Atlantic Rain Forest. *Biodiversity and Conservation* 20: 1713–1729. <https://doi.org/10.1007/s10531-011-0057-5>

- Souza-Silva M, Iniesta LFM, Ferreira RL (2020) Invertebrates diversity in mountain Neotropical quartzite caves: which factors can influence the composition, richness, and distribution of the cave communities? *Subterranean Biology* 33: 23–43. <https://doi.org/10.3897/subtbiol.33.46444>
- Valentim RF, Olivito JPR (2011) Unidade espeleológica Carajás: delimitação dos enfoques regional e local, conforme metodologia da IN-02/2009 MMA. *Espeleo-Tema* 22(1): 41–60.
- Violle C, Nemergut DR, Pu Z, Jiang L (2011) Phylogenetic limiting similarity and competitive exclusion. *Ecology Letters* 14(8): 782–787. <https://doi.org/10.1111/j.1461-0248.2011.01644.x>
- Walter DE, Krantz GW (2009) Collecting, rearing, and preparing specimens. In: Krantz GW, Walter DE (Eds) *A Manual of Acarology*, 3rd edn. Texas Tech University Press, Lubbock, 83–95.
- Webb CO, Ackerly DD, McPeck MA, Donoghue MJ (2002) Phylogenies and community ecology. *Annual Review of Ecology and Systematics* 33(1): 475–505. <https://doi.org/10.1146/annurev.ecolsys.33.010802.150448>